SYNTHESIS, CHARACTERIZATION, AND ANTI-CANCER ACTIVITY OF ZINC(II) COMPLEXES WITH A MIXTURE OF 1H-TETRAZOLE LIGANDS-(BENZYLTHIO)-5LICATES AND PHOSPHINES AND THEIR BIOLOGICAL ACTIVITY

A.H. Ali

Ministry of education, General Directorate of education in Salah All-din
e-mail: alaa.hamad7289@gmail.com

Received 12.01.2026
Accepted 06.03.2026

Abstract: *The research included a study of the preparation and identification of the ligand and its complexes, where 1H-tetrazole ligand-(benzylthio)-5 was used in the preparation to obtain the complexes represented by $[ZnL_2(PPh3)_2Cl]Cl$, $[Zn_2L_4(\mu\text{-}dppm)_2]Cl_4$, $[ZnL_2(dppp)]Cl_2$ (where dppm = bis(diphenylphosphino)methane and dppp = 1,3-bis(diphenylphosphino)propane). The prepared compounds were studied, and their identities were determined by FT-IR spectroscopic properties. ^{1}H-NMR, ^{31}P-NMR spectra, and scanning electron microscopy (SEM) showed that the ligand coordinates by coordination occurs through the nitrogen atom of the tetrazole ring and the phosphorus atoms of the phosphine through the phosphorus atom P. The biological activity, including antibacterial and anticancer, was evaluated. This study contributes to the development of new metal complexes with distinct biological activity.*
Keywords*: Triazole, phosphines, biological effectiveness, anti-cancer, zinc(II) complexes.*

1. Introduction

Tetrazoles are heterocyclic organic compounds consisting of a five-membered ring containing one carbon atom and four nitrogen atoms in addition to hydrogen. Their molecular formula is CH_2N_4. They are yellow solids with a distinctive odor and are soluble in water and alcohol [1]. They are widely used in the pharmaceutical field, due to their biological activity [2]. Tetrazoles exist in two tautomeric formulas.

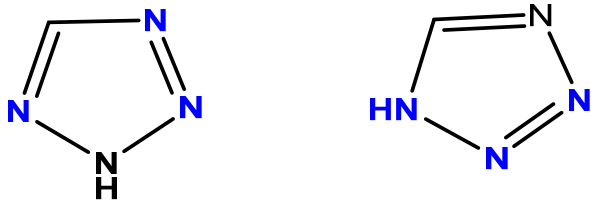

The most common method of preparing the tetrazole ring is by adding hydrazoic acid or azide to compounds that react with compounds containing a C≡N group, such as carbodi-imines, cyanates, thiocyanates, and cyanides. During this reaction, an imidoyl azide intermediate is formed, which undergoes ring closure to form the tetrazole ring [3], as shown below:

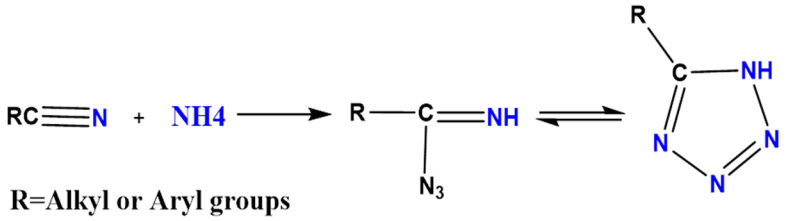

Tetrazole biolodical activity: Compounds containing the tetrazole ring have occupied a wide space in the field of pharmaceutical compounds, as this ring is used in the composition of a number of antibiotics such as (a) *Cefazolin* [4] and (b) *Ceftazole* [5], as in Fig. 1.

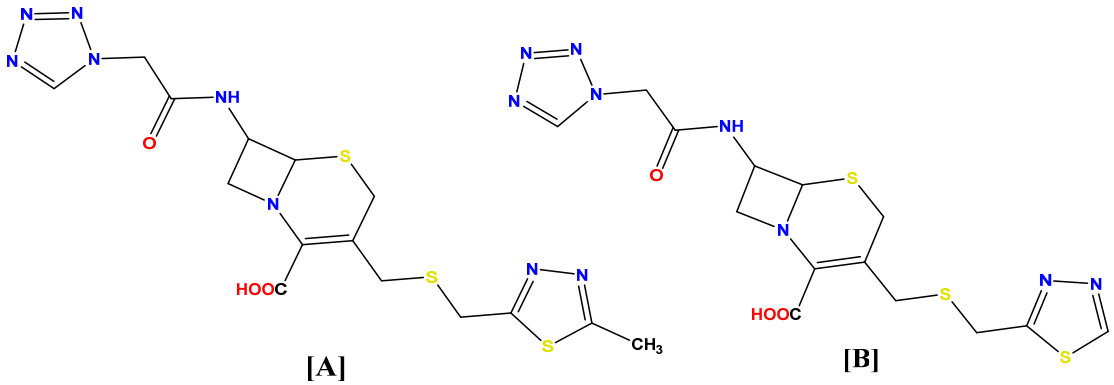

Fig. 1. Structure of (A) *Cefazolin* [4] and (B) *Ceftazole* [5]

Tetrazoles exhibit broad biological activities, as they have been used as analgesics, antimicrobials, antibacterials, and anticancer agents. Compounds (A) and (B) have an antidiabetic effect [6], and compound (C) has an antimicrobial effect, and compound (D) has an antibacterial effect [7] (Fig. 2).

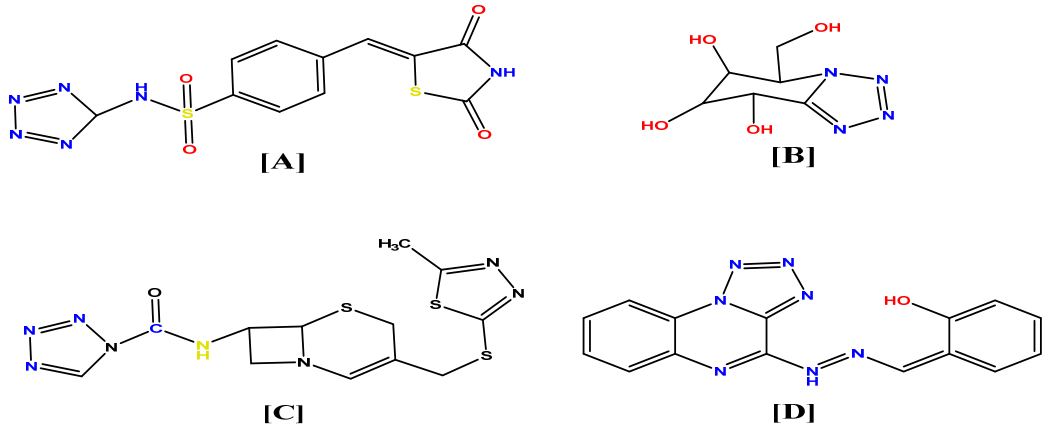

Fig. 2. Structure of compounds [A], [B], [C] and [D]

2. Experimental Part

All chemicals and solvents were used as received without further purification, and all of these materials were provided by Sigma-Aldrich and Fluka Analytical. The melting points of the compounds were measured using a Stuart melting point apparatus. In terms of the infrared spectra, they were captured using a SHIMADZU FT-IR-8400s spectrophotometer, in the range of 400-4000 cm^{-1}, with samples prepared as KBr tablets. Spectra of ^{1}H-NMR, ^{13}C-NMR, and ^{31}P-NMR were obtained using a Bruker instrument operating at a frequency of 400 MHz, employing (DMSO-d^{6}) as the solvent. Its various crystalline dimensions of the particles were determined using the (TESCAN MIRA3) scanning electron microscope.

2.1 Methods

2.1.1 Preparation of $[Zn(L)_2]Cl_2$. A hot, colorless solution of zinc chloride (0.1 g, 0.31 mmol) in 5 ml of ethanol was added to the solution of ligand L (0.129 g, 0.62 mmol) in 5 ml. A white precipitate formed. The mixture was heated to 80°C. The precipitate was filtered and washed with cold ethanol; the precipitate was allowed to dry at room temperature. The prepared compound had the following physical properties (wt=0.14 g, %=77%, m.p.=182-184°C).

2.2 Synthesis of $[ZnL_2(PPh_3)_2Cl]Cl$ and complexes $[Zn_2L_4(\mu\text{-dppm})_2]Cl_4$, $[ZnL_2(dppp)]Cl_2$. A solution of ligand L (0.1 g, 0.5 mmol) in 5 ml of ethanol was added to a solution of zinc chloride ($ZnCl_2$) (0.16 g, 0.86 mmol) in 5 ml of ethanol. A milky mixture was formed. The solution was submerged at 70°C for 2 hours. Then PPh_3 (0.13 g, 0.5 mmol) in 5 ml of ethanol was added to the mixture. The mixture was stirred under reflux for 2 hours. After filtering the precipitate

while it was still hot, the product was washed with cold ethanol and dried at room temperature. The prepared compound had the following physical properties. (wt = 0.08 g, % = 50%, m.p.= 160-163°C)

Phosphine = dppm, dppp. Ligand L (0.129 g, 0.62 mmol) and zinc chloride (0.1 g, 0.31 mmol) were added in a round-bottomed flask, and then 25 ml of chloroform was added to the mixture, forming a colorless solution. It was heated for 2 hours at 50°C to form a milky suspension. Then add a 0.119 g (0.31 mmol) dppm solution in 5 ml of chloroform and heat the mixture at 70°C for 2 hours to form a colorless solution. The solution was allowed to evaporate at room temperature. The prepared compound had the following physical properties (wt=0.18 g, %=60%, m.p.=194-196°C).

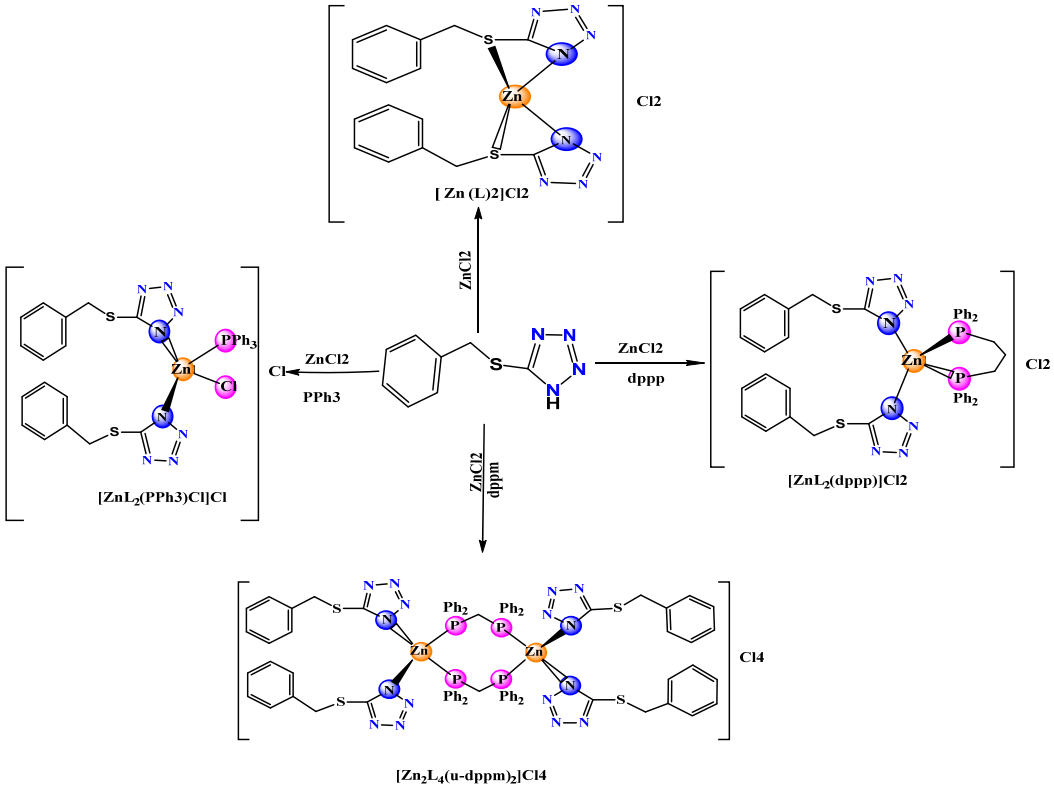

Scheme 1. Preparation of Complexes

[Zn(L)$_2$]Cl$_2$ (1) white powder, yield (0.14 g, 77.70%), IR (KBr, cm^{-1}): melting point=178°C; 3058 ν (C-H) aromatic, 2991m ν (C-H)Alephate, 1620s ν (C=N), 1346m ν (N=N), 1242s ν (N=N), 769m ν (C-S), 422w ν (M-P). ^{1}H-NMR (δppm, *J*Hz, DMSO-*d*^{6}), **δ**=7,46 (d, ^3J = 7.88 Hz, 4H, Ha), 7.35 (t, ($^4J_{H-H}$= 7.70 Hz, $^3J_{H-H}$= 1.20 Hz) 4H, Hb), 7.20 (d, $^4J_{H-H}$= 7.66 Hz,$^3J_{H-H}$= 1.16 Hz, 2H, Hc), 3.91(s, 4H, CH$_2$). ^{13}C-{^{1}H}-NMR: 161.05 (C=N), 149.07 (C=C), 129.11(N-C), 38.82 (CH$_2$). Elemental analysis calculated for $C_{16}H_{14}N_8ZnS_2Cl_2$: C, 33.21; H, 2.93; N, 16.31; S, 9.33. Found: C, 35.43; H, 2.77; N, 6.62. Cl, 8.62. Λ (Ω^{-1}.cm^2. mol^{-1}): 128.74. Λ (Ω^{-1}.cm^2. mol^{-1}): 38.42.

[Zn$_2$(L)$_2$(PPh$_3$)Cl]Cl (2) white powder, yield (0.41g, 86%), IR (KBr, cm-1): melting point=170°C; 3068m ν(C-H)Arom, 2999m ν(C-H)aliph, 1620s ν(C=N), 1589s ν(C=C), 1436s ν(P-Ph), 1242s ν(N-N), 750s ν(C-S), 696m ν(P-C), 424s ν(M-P). ^{31}P-{^{1}H}NMR (δppm, DMSO-*d*^{6}), **δ**=26.69(s); ^{1}HNMR (δ ppm, *J* Hz, DMSO-*d*^{6}), 7,65 (d, 3J = 8.11 Hz, 4H, Ha), 7.50 (m, 19H, Hb+3Ph), 7.35 (t, 3J = 7.56 Hz, , 3J = 1.24 Hz, 2H, Hc), 3.91 (s, 3J = 4.06 Hz, 4H, CH2). Elemental analysis calculated for $C_{52}H_{44}ZnN_8O_4P_2S_2Cl_2$: C, 56.39; H, 4.00; N, 10.12; S, 5.79; P, 5.59. Found: C, 45.26; H, 2.61; N, 5.53; Cl, 7.93. Λ (Ω^{-1}.cm^2. mol^{-1}): 52.63.

[Zn$_2$(L)$_4$(μ-dppm)$_2$]Cl$_4$ (3) white powder, yield (0.18 g, 60%). Melting point=196 °C. IR (KBr, cm^{-1}): 3053m ν(C-H)Arom, 2991m ν(C-H)aliph, 1620s ν(C=N), 1596s ν(C=C), 1434s ν(P-Ph), 1249s ν(N-N), 748s ν(C-S), 688m ν(P-C), 480s ν(M-P); ^{31}P-{^{1}H}NMR (δppm, DMSO-*d*^{6}), **δ**=29.66(s). Elemental analysis calculated for $C_{34}H_{32}Zn_2N_8P_4S_4Cl_2$: C, 30.98; H, 2.45; N, 17.00; P, 9.40; S, 9.73; Zn, 30.44. Found: C, 37.43; H, 2.94; N, 6.67; Cl, 8.55; Λ (Ω^{-1}.cm^2.mol^{-1}): 138.74.

[Zn(L)$_2$(dppp)]Cl$_2$ (4) white powder, yield (0.21 g 66%). Melting point=168 °C). IR (KBr, cm^{-1}): 3056m ν(C-H)Arom, 2996m ν(C-H)aliph, 1629s ν(C=N), 1434s ν(P-Ph), 1247s ν(N-N), 754s ν(C-S), 692m ν(P-C), 432s ν(M-P). ^{31}P-{^{1}H}NMR (δppm, DMSO-d^6), **δ**=28.13(s). Elemental analysis calculated for $C_{22}H_{20}N_8ZnP_2S_2Cl_2$: C, 33.21; H, 2.93; N, 16.31; P, 9.02; S, 9.33; Cl, 7.68. Λ (Ω^{-1}.cm^2. mol^{-1}): 75.42.

3. Results and Discussion

3.1. Conductivity measurements and elemental analysis: The molar conductivity values suggest 1:1 (zinc ion:Ligand L:PPh$_3$), 1:4 (zinc ion:Ligand L:dppm), and 1:2 (zinc ion:Ligand L:dppp). The outcomes confirmed that the methods used to create the mixed ligand complexes yielded highly pure materials. The resulting complexes were slightly soluble in acetone, ethanol, and methanol solvents but completely soluble in DMF or DMSO. Despite using a variety of solvents and recrystallization methods, all attempts to create suitable crystals for crystallographic studies were unsuccessful.

3.2. FTIR Spectra. The infrared spectrum of the [L] complex showed a strong band in the range (1625-1620 cm^{-1}) that is attributed to the stretching frequency of the (C=N) group within the five-membered ring [8]; a powerful band in the range (1340-1350 cm^{-1}) that is attributed to the stretching of the (N=N) group [9, 10] as evidence of the formation of the ligand; a band in the range (750-765 cm^{-1}) that is attributed to the stretching of the (C-S) group (12); along with a band at (1240-1250 cm^{-1}) that is attributed to the stretching of (N-N) [11]. As shown in Fig. 3.

The [Zn(L)$_2$Cl$_2$] complex's infrared spectrum revealed a sharp and strong band in the range (1620 cm^{-1}) that is ascribed to the stretching frequency of the (C=N) group among the five-membered ring [8], a sharp and strong band in the range (1346 cm^{-1}) that is attributed to the stretching of the (N=N) group [10] as evidence of the ligand's formation, a band in the range (769 cm^{-1}) that is attributed to the stretching of the (C-S) group [12], and a band at (1242 cm^{-1}) that is attributed to the extension of (N-N) [11]. As shown in Fig. 4.

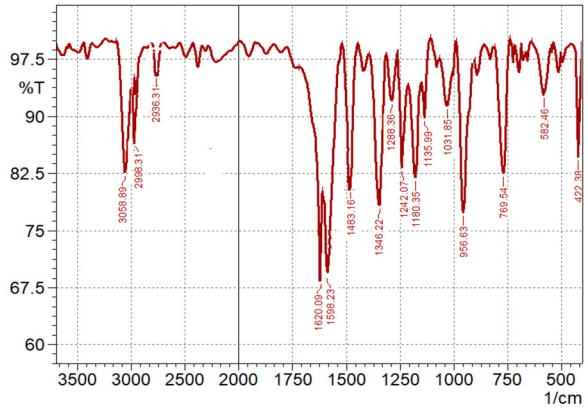

Fig. 3. IR spectrum of the ligand [L]

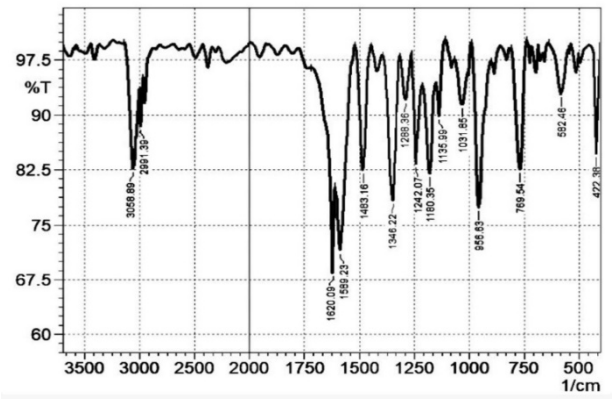

Fig. 4. IR spectrum of the [Zn(L)$_2$]Cl$_2$

The [Zn(L)$_2$(PPh$_3$)Cl]Cl complexes' infrared spectrum revealed two distinct bands that were absent from the ligand's infrared spectrum in the range (1031 cm^{-1}) attributed to (C-P) and a band in the range (1436 cm^{-1}) [13-16] attributed to the phosphine groups' vibrational frequency (Ph-P)^2 [17]. The stretching regularity of the five-membered ring's (C=N) group (8) is responsible for the spectrum's sharp and strong band in the range of 1620 cm^{-1}, and The expansion of the (N=N) group (10) is responsible for the appearance of a sharp and strong band in the range of 1483 cm^{-1}, which is evidence of the ligand's formation and the emergence of a band in the 769 cm^{-1} range. It was explained by the C-S group's stretching [12], along with the formation of a band at 1242 cm^{-1}, which is caused by the stretching of N-N [11].

The $[Zn_2(L)_2\mu\text{-}(dppm)_2]Cl_4$ complexes' infrared spectrum. The stretching vibration of the ν(Ph-P) group [17] was responsible for the appearance of a band in Cl_4 with a frequency of 1436 cm^{-1}, while the stretching of the ν(C-N) group [18] was responsible for a band at 1242 cm^{-1}. Additionally, two new bands that were absent from the free ligand's spectrum (1099 cm^{-1}, 769 cm^{-1}) appeared between the spectra and were attributed to the vibrational frequency of the ν(C-P) group [15, 16]. The stretching frequency of the (C=N) group within the pentagonal ring is responsible for the spectrum's strong, crisp band in the range of 1620 cm^{-1} [8]. Additionally, the emergence of a sharp and powerful band within the range (1348 cm^{-1}) was attributed to the elongation of the ligand's creation, demonstrated by the (N=N) group [10], and the continuation of the (C-S) group [12] was responsible for the emergence of a band within the range (669 cm^{-1}), while the stretching of (N-N) was responsible for a band's arrival at (1242 cm^{-1}) [11]. As shown in Fig. 5.

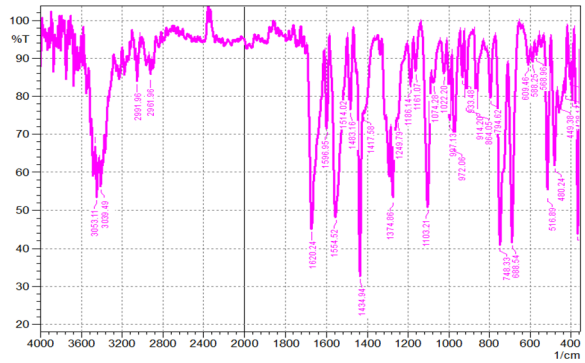

Fig. 5. IR spectrum of $[Zn_2(L)_2(\mu\text{-}dppm)_2]Cl_4$

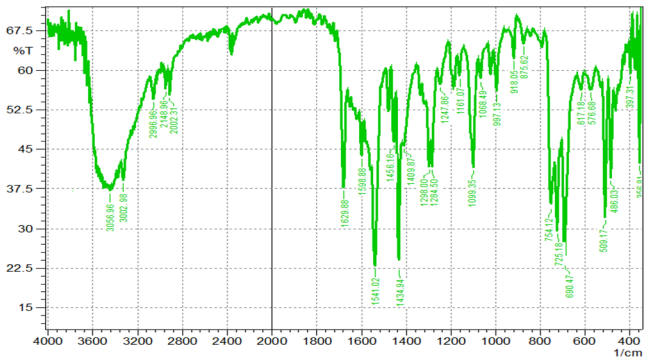

Fig. 6. IR spectrum of $[Zn(L)(dppp)]Cl_2$

The $[Zn(L)_2(dppp)]Cl_2$ complexes' infrared spectrum. The stretching of the ν(Ph-P) group [17] was responsible for the appearance of a band in the frequency range of 1434 cm^{-1} in Cl_2, while the stretching of the ν(C-N) group [18] was responsible for a band's arrival at 1247 cm^{-1}. Two new bands that were absent from the free ligand's spectrum (1099 cm^{-1}, 752 cm^{-1}) were ascribed to the vibrational frequency of the ν(C-P) group [15, 16]. The frequency at which the (C=N) group stretches within the pentagonal ring is responsible for the spectrum's strong, crisp band in the range of 1629 cm^{-1} [8]. A band within the range (1554 cm^{-1}) [9] was also shown, due to the (C=C) vibration group in the ligand, as well as the emergence of a strong, sharp band in the vicinity (1340-1355 cm^{-1}), which was ascribed to the ν(C-P) group's stretching [16]. In addition to a band's appearance at 1250-1240 cm^{-1} caused by the stretching of N-N [11-13]. As shown in Fig. 6.

3.3. NMR spectra. The CH_2 group's protons and an integration of four protons were responsible for a single signal at δH = 3.92 ppm in the ^{1}H-NMR spectra of ligand (L) in dMSO-d_6 solvent. The (Ha) proton and an integration of four protons were identified as the sources of two signals at the chemical shift (**δ**H = 7.60 ppm) with a coupling constant (^{3}JHa-Hb = 7.50 Hz). Additionally, the ligand's spectra revealed a triple signal at (**δ**H = 7.40 ppm) with a coupling constant (^{3}JHb - Hc = 7.80 Hz) ascribed to an integration of four protons and the (Hb) proton. As seen in Fig. 7, a triple signal at δH = 7.25 ppm with a coupling constant ^{3}JHb-Hc = 7.62 Hz was assigned to a proton (Hc) by an integration that shows two protons.

The carbon atom of the (CH_2) group was identified as the source of a signal at the shift (δH = 38.82 ppm) in the ligand's ^{13}C-{^{1}H}-NMR spectrum. Additionally, it displayed a signal at the shift (**δ**H = 129.11 ppm) that was ascribed to the tetrazole ring's (N-C) group. Additionally, the carbon atom (C=C) in the benzene ring was identified as the source of a signal at (H = 149.07 ppm), while the carbon atom (C=N) in the tetrazole was identified as the source of a signal at (H = 161.05 ppm). As seen in Fig. 8, the remaining signals of the carbon atoms in the ligand occurred in the range (**δ**H = 121.20, 125.19 ppm).

Just one signal during the shift (**δ**H = 3.91 ppm) in the ligand's proton nuclear magnetic resonance (^{1}H-NMR) spectrum $[Zn(L)_2]Cl_2$ recorded in dMSO-d_6 solvent was allocated to the CH_2 group's protons and an integration of four protons. The (Ha) proton and an integration of four protons appeared as two doublets at the chemical shift (**δ**H = 7.45 ppm) with a coupling constant (^{3}JHa-Hb = 7.49 Hz). Additionally, the ligand's spectra had a triple signal at (δH = 7.35 ppm), which was identified as the (Hb) proton with an integration of four protons.

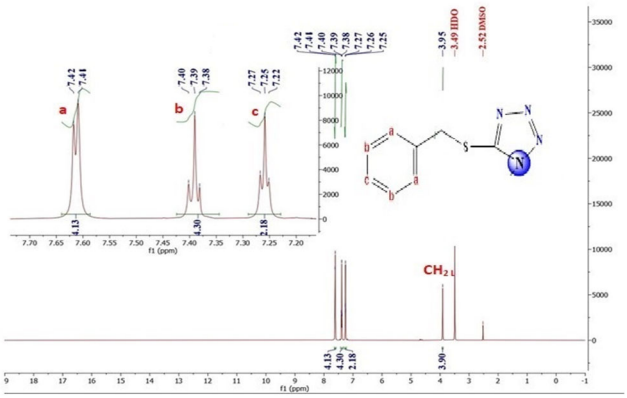

Fig. 7. ^{1}H-NMR spectrum of the liganed [L]

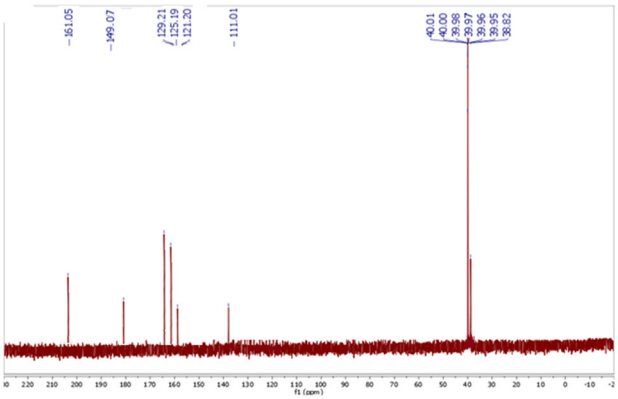

Fig. 8. ^{13}C-{^{1}H}-NMR spectrum of the liganed [L]

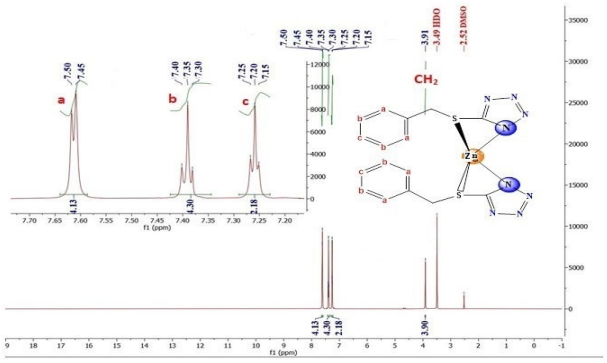

Fig. 9. ^{1}H-NMR spectrum of the liganed $[Zn(L)_2(PPh_3)Cl]Cl$

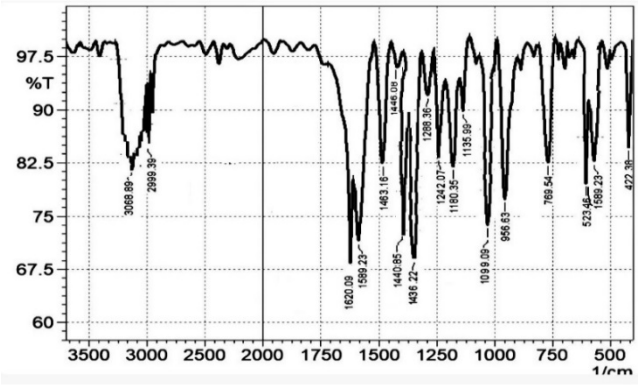

Fig. 10. ^{31}P-{^{1}H}-NMR spectrum of $[Zn(L)_2(PPh_3)Cl]Cl$

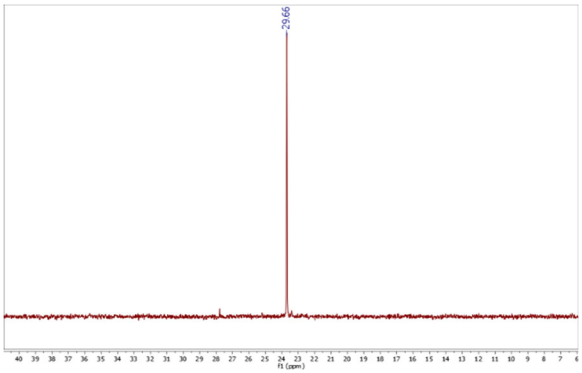

Fig. 11. ^{31}P-{1H}-NMR spectrum of $[Zn_2(L)_2$ $[Zn(L)(dppp)]Cl_2$

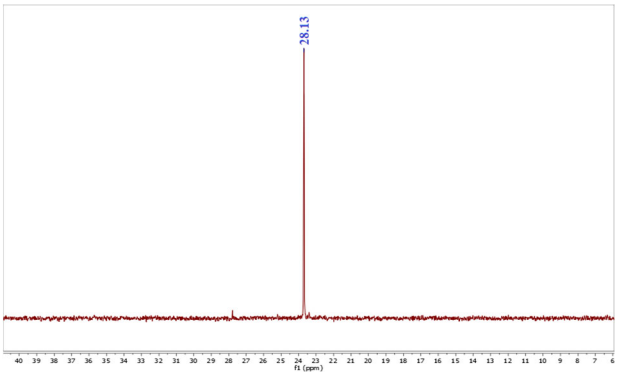

Fig. 12. ^{31}P-{1H}-NMR spectrum of $(\mu$-dppm$)_2]Cl_4$

The ligand's proton nuclear magnetic resonance (^{1}H-NMR) spectrum of $[Zn(L)_2(PPh_3)Cl]Cl$, measured in dMSO-d_6 solvent, revealed an integration of four protons and a single signal at the shift (**δ**H = 3.91 ppm) attributed to the protons of the CH_2 group. The (Ha) proton and an integration of four protons were identified as the sources of two signals at the chemical shift (**δ**H = 7.63 ppm) with a coupling constant (^{3}JHa-Hb = 7.48 Hz). Additionally, a multiple signal at (δH = 7.50 ppm) in the ligand's spectra was identified as the (3Ph + Hb) proton with an integration of 19 protons (Fig. 9).

The $[Zn(L)_2(PPh_3)Cl]Cl$ complex's ^{31}P-{^{1}H}NMR spectra showed a singlet with zinc satellites at (δP=26.69 ppm). Similar to complexes in Figure 10, this singlet supports the proposed structure of the complex by confirming the analogous nature of the phosphorus atoms in **PPh_3**.

The $[Zn_2(L)_2(\mu\text{-dppm})_2]Cl_4$ complex's ^{31}P-{^{1}H}NMR spectra showed a singlet with zinc satellites at (δP=29.66 ppm). Similar to the complex in Figure 11, this singlet supports the suggested structure of the complex by indicating the analogous nature of the phosphorus atoms in **dppm**.

The $[Zn(L)(dppp)]Cl_2$ complex's ^{31}P-{^{1}H}NMR spectra showed a singlet with zinc satellites at (δP=28.13 ppm). Similar to the complex in Fig. 12, this singlet supports the suggested structure of the complex by indicating the analogous nature of the phosphorus atoms in **dppp**.

3.4. Anti-cancer study. FAS 100 and 89 were tested for their anti-cancer effects on cancer cells using MTT [4,5-2,5-diphenyltetrazolium bromide (dimethylthiazole-2-yl)]. They diluted the stock solutions to the necessary concentrations after the FAS $[Zn_2(L)_4(\mu\text{-dppm})_2]Cl_4$ and $[Zn_2(L)_2(PPh_3)Cl]Cl$ were dissolved in DMSO. The anti-tumor efficacy of the substances was evaluated using the 518A2 melanoma cancer cells. A 96-well plate was filled with cancer cells. The FAS 100 and 89 were introduced at doses of 0.1 µM, 1 µM, 10 µM, 100 µM, 200 µM, and 400 µM after a 24-hour incubation period. DMSO served as the negative control. The MTT test was given 48 hours after the start of therapy. In short, each well received 100 µL of brand-new medium. after the medium was taken out of the 96-well plate. After adding 10 µL of the previously made stock solution of 12 mM MTT (SERVA) and incubating for four hours at 37 °C, each well was given a 0.01 M SDS-HCl solution in 100 µL. After four more After being incubated for hours, the samples were combined using a pipette, and then the absorbance at 570 nm was determined. For statistical analysis, the experiments were conducted three times [18]. The mixed ligand Zn(II) complexes $[Zn_2(L)_4(\mu\text{-dppm})_2]Cl_4$ and $[Zn_2(L)_2(PPh_3)Cl]Cl$ have anticancer properties. An MTT assay using 3-(4,5-dimethylthiazol-2-yl)-2,5-diphenyl tetrazolium bromide was used to evaluate Cl against 518A2 cancer cell lines. Tables 1 and 2 and Figure 13 display The quantities of the investigated chemicals needed for IC50, or 50% inhibition of the cells, and compare the outcomes as a positive control using cis-platin. $[Zn_2(L)_4(\mu\text{-dppm})_2]$ With an IC50 value of 53.01 ± 6.22 µM, Cl_4 exhibited the strongest activity against 518A2, while $[Zn_2(L)_2(PPh_3)Cl]$ With an IC50 value of 173.40 ± 5.56 µM, Cl showed a poor anti-cancer effect against similar cell lines.

Table 1. Cell viability (%) of compounds FAS 100 and 89 against 518A2 cell line

Concentrated (µM)	Cell survival (%)*	
	B4	S3
0.000	100	100
0.100	100	94.50
1.000	94.71	87.56
10.00	86.96	74.26
100.0	72.10	50.89
200.0	45.97	24.30
400.0	16.25	14.34
**These figures represent the mean of three replicates.*		

Table 2. IC_{50} values of compounds FAS 100 and 89 against 518A2 cell line in comparison to cis-platin

Compound	IC_{50} value (µM)
$[Zn2(L)_4(\mu\text{-dppm})_2]Cl_4$	53.01 ± 6.22
[Zn2(L)2(PPh3)Cl]Cl	173.40 ± 5.56
Cis-platin	1.45 ± 0.04

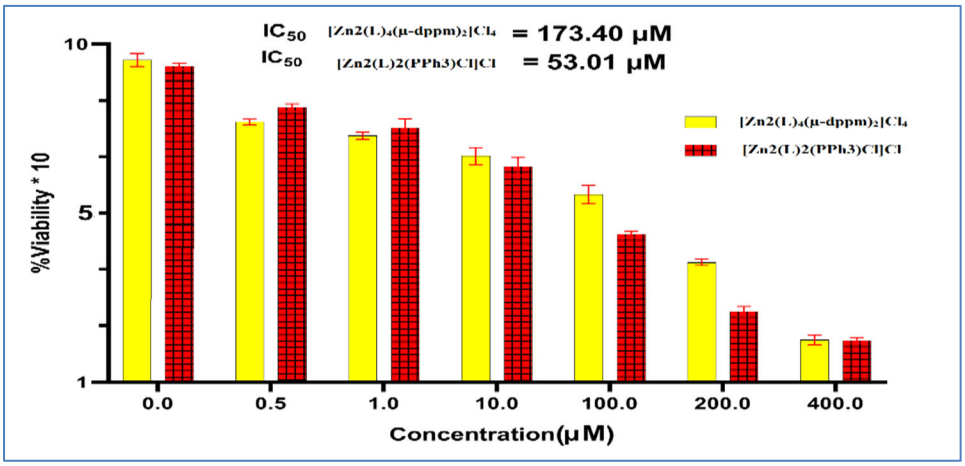

Fig. 13. MCF-7 cell viability following FAS 100 and 89 treatment at varying doses (M). P value in each instance is 0.005

3.5. SEM study. The majority of coordination complexes can be created with regular geometric structures at nanoscale levels, according to recent research on their geometric structure [19]. SEM was used to examine the microstructure's morphological appearance in a few of the produced complexes (Fig. 14). The $[Zn(L)_2(dppp)]Cl_2$ complex's average particle size was 70 nm, which is one of the nanoparticles, according to scanning electron microscopy investigation [19, 20].

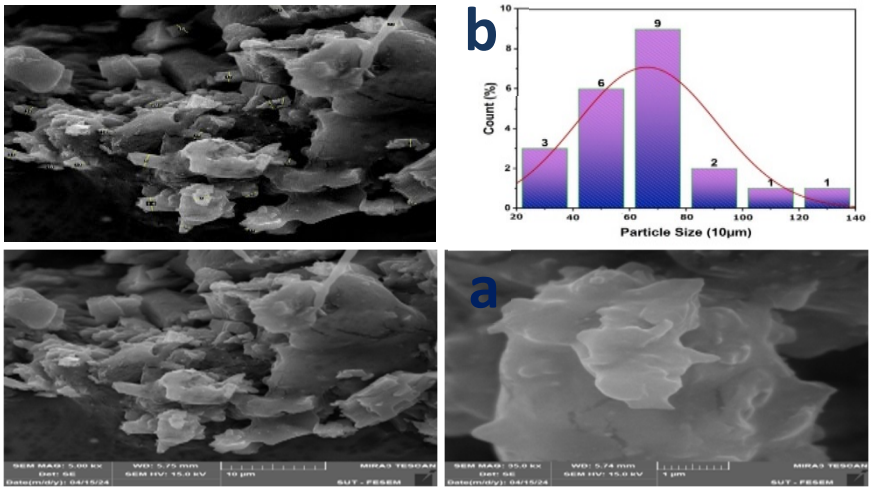

Fig. 14. ***(a)*** SEM image of the $[Zn(L)_2(dppp)]Cl_2$ complex at 1 µm and 10 µm. Graph ***(b)*** particle sizes and Gaussian curve for the $[Zn(L)_2(dppp)]Cl_2$ complex at 10 µm

3.6. Antibacterial activities. Amikacin was used as the positive control a reference to evaluate the biological activity of the complexes (0.01, 0.001, and 0.0001 mg/ml) against four bacterial species: *Escherichia coli (-), Acinetobacter baumannii*, *Staphylococcus aureus (+),* and *Enterococcus faecalis (+).* Each complex exhibited antibacterial activities against the bacterial species. Complex (1) demonstrated the highest inhibition percentage at concentration 10^{-3}. Complex (2) demonstrated the greatest inhibition % for (+) *Staphylococcus aureus and (Enterococcus faecalis) bacteria* at concentration 180, whereas complex (1) demonstrated the greatest efficacy for *Escherichia coli* bacteria at concentration 10 [21-29].

Conclusions

The ligand (5-(benzylthio)-1H-tetrazole) (L) and other mixed ligands were used to prepare the new zinc chloride complexes. The suggested formulas were $[Zn(L)_2]Cl_2$ (1), $[Zn_2(L)_2(PPh_3)Cl]Cl$ (2), $[Zn_2(L)_4(\mu\text{-dppm})_2]Cl_4$ (3), and $[Zn(L)_2(dppp)]Cl_2$ (4), where phosphine (dppm) and ligands coordinate as bridging ligands in a binuclear complex, whereas PPh_3 and dppp act as bidentate chelating ligands in a mononuclear complex. Elemental analysis, molar conductivity measurement, FTIR spectroscopy, ^{1}H-, ^{13}C-, and ^{31}P-NMR spectroscopy, and SEM were used to characterize the produced compounds.

The SEM analysis revealed that the complexes under study contained aggregates and nanocrystalline structures, with nanoscale diameters ranging from 69.9 to 154.9 nm. Every complex exhibited action against bacterial species. Complex (1) had the maximum inhibition rate for (-) *Acinetobacter baumannii*. and *(-) Escherichia coli* at concentration 10^3 whilst concentration 10 showed poor action against bacterial species. At concentration 180, complex (2) had the greatest inhibition rate for (+) *Enterococcus faecalis* and (+) *Staphylococcus aureus*. For *Escherichia coli*, complex (1) demonstrated the maximum activity at concentration 10, but complex (2) demonstrated the highest activity for the other species at the same concentration.

References

1. Popova E.A., Trifonov R.E., Ostrovskii V.A. Advances in synthesis of tetrazoles coordinated to metal ions. *Arkivoc.* 2012, **Vol. 2012(part 1)**, p. 45–65. DOI: 10.3998/ark.5550190.0013.102.
2. Alshargabi A. Diclofenac derivatives as promising anticancer and anti-inflammatory drugs: Synthesis, formulations, and pharmacokinetics. *Journal of Drug Delivery Science and Technology*, 2024, **Vol. 95**, 105544. DOI: 10.1016/j.jddst.2024.105544
3. Popov K., Volovnenko T., Volovnenko J. On the functionalization of benzo[*e*][2,1]thiazine. *Beilstein Journal of Organic Chemistry*, 2009, 5, **No. 42**. https://doi.org/10.3762/bjoc.5.42
4. Alsaiari R.A., Kamel M.M., Mohamed M.M. Corrosion inhibition of expired cefazolin drug on copper metal in dilute hydrochloric acid solution: Practical and theoretical approaches. *Molecules*, 2024, **Vol. 29(5)**, 1157. DOI: 10.3390/molecules29051157
5. Kabi A.K., Sravani S., Gujjarappa R., Garg A., Vodnala N., Tyagi U., Kaldhi D., Velayutham R., Gupta S., Malakar Ch.C. *An introduction to the evolution of azole derivatives in medicinal chemistry*. In: Swain, B.P. (eds) Nanostructured Biomaterials. Materials Horizons: From Nature to Nanomaterials. Springer, Singapore. https://doi.org/10.1007/978-981-16-8399-2_4
6. Jeyachandran M., Shiram K. Synthesis of antibacterial Ethyl 3-aryl/alkyl-2-(1H-tetrazol-5-yl)enoates and 5,5'-(2-Aryl alkene-1,1-diyl)-bis(1H-tetrazoles). *International Journal of Applied Biology and Pharmaceutical Technology*, 2011, **Vol. 2(2)**, p. 349- 353.
7. Yella R., Khatun N., Rout S., Patel B. Organic synthesis and biological evaluation of heterocyclic compounds. *Organic & Biomolecular Chemistry*, 2011, **Vol. 9**, p. 3235–3242.
8. Tisseh Z., Dabiri M., Nobahar M., Khavasi H., Bazgir A. Efficient synthesis of nitrogen-containing heterocycles. *Tetrahedron*, 2012, **Vol. 68**, p. 1769–1773.
9. Balouiri M., Sadiki M., Ibnsouda S.K. Methods for in vitro evaluating antimicrobial activity: A review. *Journal of Pharmaceutical Analysis*, 2016, **Vol. 6(2)**, p. 71–79.
10. Gonelimali F.D., Lin J., Miao W., Xuan J., Charles F., Chen M., Hatab S.R. Antimicrobial properties and mechanisms of action of plant extracts against food pathogens. *Frontiers in Microbiology*, 2018, **Vol. 9**, 389103.
11. Halder B., Middya P., Gomila R. M., Frontera A., Chattopadhyay S. Synthesis, Structural Characterization, and Theoretical Analysis of Nonconventional Bonding in Dinuclear Zinc (II) Complexes with Tridentate Schiff Bases. *ACS omega*, 2024, **Vol. 9(40)**, p. 41787-41796.
12. Sun C., Lux S., Müller E., Meffert M., Gerthsen D. Versatile applications of modern scanning electron microscopy for materials characterization. *Journal of Materials Science*, 2020, **Vol. 55**, p. 13824–13835.

13. Shaikh S.K., Kamble R.R., Somagond S.M., Devarajegowda H.C., Dixit S.R., Joshi S.D. Tetrazolylmethyl quinolines: Design, docking studies, synthesis, anticancer and antifungal evaluation. *European Journal of Medicinal Chemistry*, 2017, **Vol.128**, p. 258–273.
14. Uppadhayay R.K., Kumar A., Teotia J., Rathi I., Singh P., Ali S.K. Structural, physical, surface, and NMR studies of synthesized compounds. *Journal of Molecular Structure*, 2022, **Vol. 13(07)**, DOI: 10.47750/pnr.2022.13.S07.661
15. Tisseh Z., Dabiri M., Nobahar M., Khavasi H., Bazgir A. Efficient synthesis of nitrogen-containing heterocycles. *Tetrahedron*, 2012, **Vol. 68**, p. 1769–1773.
16. Balouiri M., Sadiki M., Ibnsouda S.K. Methods for in vitro evaluating antimicrobial activity: A review. *Journal of Pharmaceutical Analysis*, 2016, **Vol. 6(2)**, p. 71–79.
17. Gonelimali F.D., Lin J., Miao W., Xuan J., Charles F., Chen M., Hatab S.R. Antimicrobial properties and mechanisms of action of plant extracts. *Frontiers in Microbiology*, 2018, **Vol. 9**, 389103.
18. Mohammed A., Abdullah A. Scanning electron microscopy (SEM): A review. *Proceedings of the International Conference on Hydraulics and Pneumatics (HERVEX)*. 2018. p. 7–9.
19. Sun C., Lux S., Müller E., Meffert M., Gerthsen D. Versatile applications of modern scanning electron microscopy. *Journal of Materials Science*, 2020, **Vol. 55**, p. 13824–13835. DOI: 10.1007/s10853-020-04970-3
20. Shaikh S.K., Kamble R.R., Somagond S.M., Devarajegowda H.C., Dixit S.R., Joshi S.D. Tetrazolylmethyl quinolines: Design, docking studies, synthesis, anticancer and antifungal evaluation. *European Journal of Medicinal Chemistry*, 2017, **Vol. 128**, p. 258–273. DOI: 10.1016/j.ejmech.2017.01.043
21. Shawkat S.M., Talluh A.A., Khairallah B.A., Saleh M.J., Saleh J.N., Abdulmajeed A.Z., Ibrahim L.D. Preparation and characterization of new thiazolidine-4-one derivatives and evaluation of their bactericidal activity. *Results in Chemistry*, 2026, **Vol. 26**, 103339.
22. Muhammad F.M., Khairallah B.A., Albadrany K.A. Synthesis, characterization and antibacterial evaluation of novel 1,3-oxazepine derivatives using a cycloaddition approach. *Journal of Angiotherapy*, 2024, **Vol**. **8(3)**, p. 1–9.
23. Ahmed S.E., Ghanim Ahmed Z.A., Mustafa G.S., Saleh M.J., Saleh J.N. Preparation and characterization of new azetidine rings and evaluation of their biological activity. *Advanced Journal of Chemistry, Section A*, 2026, **Vol**. **9(1)**, p. 146–154.
24. Noman R.S., Ahmed S.E., Ahmed N.A.A., Saleh M.J., Saleh J.N. Synthesis, characterization, and biological evaluation of novel tetrazole-derived compounds. *Advanced Journal of Chemistry, Section A*, 2026, **Vol**. **9(5)**, p. 940–946.
25. Al-Joboury W.M.R., Sulaiman R.Z., Saleh M.J., Al-Badrany K.A., Saleh J.N. Preparation and characterisation of azetidine-4-one compounds and evaluation of their antibacterial activity. *Oxidation Communications*, 2025, **Vol**. **48(4)**, p. 1582–1594.
26. Abdullah S.H., Saber A.B., Al-Badrany K.A., Saleh J.N., Saleh M.J. Synthesis, characterization, enzymatic activity of some pyrazoline derivatives, azo dyes, and chalcones derived from ethyl 4-(trifluoromethyl) benzoate. *Chemical Problems*, 2026, **Vol. 24(3)**, p. 346–361.
27. Najm R.S., Saleh M.J., Saleh J.N. Synthesis and Characterization of New Graphene Nanocomposites and Study of Their Antibacterial, Antifungal and Anticancer Activity. *Chemical Problems*, 2026, **Vol. 24(3)**, p. 333–345.
28. Najm R.S., AL-Rasheed A.A., Mohammed A.S., Garba B., Saleh M.J. Synthesis, chemical characterization and biological activity evaluation of lamb meat-derived nanocomposite. *Advanced Journal of Chemistry, Section A*, 2025, **Vol. 8(12)**, p. 1890–1903.
29. Talluh A.W.A.S., Saleh M.J., Saleh J.N. Synthesis, characterization, and evaluation of biological and laser activities of some novel azetidinone derivatives. *Chemical Problems*, 2026, **Vol. 24(2)**, p. 288–295. DOI: 10.65382/2221-8688-2026-2-288-295